Quarkonium decays into an Invisible ALP

L. di Luzio, X. Ponce Diaz, A.W.M. Guerrera and S. Rigolin*

Department of Physics and Astronomy University of Padova and INFN Padova, Via Marzolo 8, Padova, Italy

Abstract

In this talk ALP production from quarkonium meson decays is presented. To this purpose, the relevant cross-section is computed via an effective Lagrangian with simultaneous ALP couplings to b-quarks and photons. The interplay between resonant and non-resonant contributions is shown to be relevant for experiments operating at $\sqrt{s} = m_{\Upsilon(nS)}$, with $n = 1, 2, 3$, while the non-resonant one dominates at $\Upsilon(4S)$. These effects imply that the experimental searches performed at different quarkonia resonances are sensitive to complementary combinations of ALP couplings. To illustrate these results, constraints from existing BaBar and Belle data on ALPs decaying into invisible final states are derived. Constrains from the recent BESIII measurement of the $J/\Psi \to \gamma\, a$ decay rate are also included for comparison.

1 Introduction

Light pseudoscalar particles naturally arise in many extensions of the Standard Model (SM), including the ones endowed with an approximate global symmetry spontaneously broken at a given scale, f_a. Sharing a common nature with the QCD axion [1,2,3], (pseudo) Nambu-Goldstone bosons are generically referred to as Axion-Like Particles (ALPs). The ALP mass m_a can, in general, be much lighter than the symmetry breaking scale f_a, as it is paradigmatically exemplified in the KSVZ and DFSZ invisible axion models [4,5,6,7]. Therefore, it may be not inconceivable that the first hint of new physics at (or above) the TeV scale could be the discovery of a light pseudoscalar state.

In this talk the existing BaBar and Belle flavor-conserving constraints on ALPs are carefully examined. In fact, the resonant contributions to the ALP production, via the $e^+e^- \to \Upsilon(nS) \to a\gamma$ process, have been previously overlooked. As will be shown, these effects can induce numerically significant corrections to experimental searches performed at $\sqrt{s} = m_{\Upsilon(nS)}$, with $n = 1, 2, 3$. A detailed analysis of these effects can be found in [8]. In order to assess the limits on ALP couplings, one should specify not only the ALP production mechanism, but also its decay products. Here, it will be assumed that the ALP does not decay into visible particles. Such a scenario can be easily achieved by assuming a sufficiently large ALP coupling to a stable dark sector, as motivated by several dark matter models. The conclusions related to ALP production are, however, general and they can also be applied to the reinterpretation of experimental searches with visible decays in the detector [9].

1.1 ALP effective Lagrangian

The dimension-five effective Lagrangian describing ALP interactions, above the electroweak symmetry breaking scale, can be generically written as [10]

$$\begin{aligned}\delta\mathcal{L}_{\text{eff}} = \frac{1}{2}(\partial^\mu a)\,(\partial_\mu a) - \frac{m_a^2}{2}a^2 - \frac{c_{aBB}}{4}\frac{a}{f_a}\,B^{\mu\nu}\widetilde{B}_{\mu\nu} - \frac{c_{aWW}}{4}\frac{a}{f_a}\,W^{\mu\nu}\widetilde{W}_{\mu\nu} \\ - \frac{c_{agg}}{4}\frac{a}{f_a}\,G_a^{\mu\nu}\widetilde{G}^a_{\mu\nu} - \frac{\partial_\mu a}{2f_a}\sum_f c_{aff}\,\overline{f}\gamma^\mu\gamma_5 f\,,\end{aligned} \tag{1}$$

where $\widetilde{V}^{\mu\nu} = \frac{1}{2}\,\varepsilon^{\mu\nu\alpha\beta}V_{\alpha\beta}$, c_{aff} and c_{aVV} denote the ALP couplings to fermions and to the SM gauge bosons, $V \in \{g, B, W\}$, respectively. The ALP mass m_a and the scale f_a are assumed to be independent parameters, in contrast to the QCD-axion paradigm, which is characterized by the relation $m_a\, f_a \approx m_\pi\, f_\pi$.

At the energy-scales relevant at B-factories, the ALP interactions with the Z boson can be safely neglected, due to the Fermi constant suppression. Furthermore, the ALP couplings to the top-quark and $W^\pm$ boson are relevant only to the study of flavor-changing neutral currents observables, which are complementary to the probes discussed here. The only relevant couplings in Eq. (1) at low-energies are

$$\begin{aligned}\delta\mathcal{L}_{\text{eff}} \supset \frac{1}{2}(\partial^\mu a)\,(\partial_\mu a) - \frac{m_a^2}{2}a^2 \\ - \frac{c_{a\gamma\gamma}}{4}\frac{a}{f_a}F_{\mu\nu}\widetilde{F}_{\mu\nu} - \frac{c_{agg}}{4}\frac{a}{f_a}\,G_a^{\mu\nu}\widetilde{G}^a_{\mu\nu} - \frac{\partial_\mu a}{2f_a}\sum_f c_{aff}\,\overline{f}\gamma^\mu\gamma_5 f\,,\end{aligned} \tag{2}$$

where $c_{a\gamma\gamma} = c_{aBB}\,\cos^2\theta_W + c_{aWW}\,\sin^2\theta_W$. The couplings relevant to ALP production are $\{c_{a\gamma\gamma}, c_{abb}\}$, while the other couplings only contribute to the ALP branching fractions.

Light pseudoscalar particles can also act as portals to a light dark sector. In this case, to describe these additional interactions, new couplings are customarily introduced. By assuming, for instance, an extra light and neutral dark fermion state χ, the following term should be considered in the effective Lagrangian:

$$\delta\mathcal{L}_{\text{eff}} \supset -c_{a\chi\chi}\,\frac{\partial_\mu a}{2f_a}\,\overline{\chi}\gamma^\mu\gamma_5\chi\,, \tag{3}$$

where $c_{a\chi\chi}$ denotes a generic coupling, which can induce a sizable ALP decay into invisible final states, as will be considered in the following.

The main goal of this talk will be to revisit the theoretical expressions available in the literature, including ALP coupling to bottom quarks[a], as well as previously unaccounted experimental uncertainties [8]. In the following, the *invisible ALP* scenario will be considered, i.e the scenario in which the coupling to the dark sector $c_{a\chi\chi}$ is large, in comparison to the SM couplings, and therefore the ALP will decay predominantly into an invisible channel, providing the mono-γ plus missing energy signature.

1.2 B-factories probes of invisible ALPs

Three different ALP production mechanisms can be identified at B-Factories.

Non-resonant ALP Production. The most straightforward way of producing ALPs in e^+e^- facilities is via the non-resonant process $e^+e^- \to \gamma a$, as illustrated in Fig. 1. If the ALP does not decay inside the detector, or decay invisibly, this process would result in an energetic γ plus missing energy. The total cross-section, keeping explicit the ALP mass dependence, is

$$\sigma_{\text{NR}}(s) \;=\; \frac{\alpha_{\text{em}}}{24}\frac{c_{a\gamma\gamma}^2}{f_a^2}\left(1 - \frac{m_a^2}{s}\right)^3\,. \tag{4}$$

[a] The case of ALP coupling to charm quarks will be shortly discussed at the end of the talk.

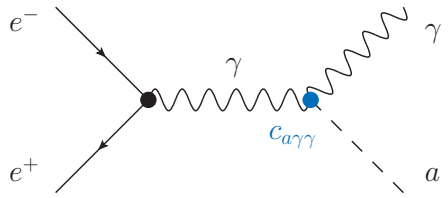

Figure 1 – *Non-resonant contribution to the process $e^+e^- \to \gamma a$ produced via the effective coupling $c_{a\gamma\gamma}$ defined in Eq.* (2).

The contributions coming from the exchange of an off-shell Z boson, which are also induced by c_{aWW} in Eq. (1), have been neglected, since they are suppressed, at low-energies, by $s/m_Z^2 \ll 1$.

While the non-resonant contribution to ALP production given above is unavoidable in any experiment relying on e^+e^- collisions, the situation at B-factories is more intricate since these experiments operate at specific $\Upsilon(nS)$ resonances. Therefore, it is crucial to account for the resonantly enhanced contributions, which can be numerically significant.

Resonant ALP Production. Vector quarkonia can produce significant resonant contributions to the mono-γ channel, $e^+e^- \to \Upsilon \to \gamma a$, since they are very narrow particles coupled to the electromagnetic current. Assuming a fixed center-of-mass energy $\sqrt{s} \approx m_\Upsilon$, as is the case at B-factories, and using the Breit-Wigner approximation, one finds for the resonant cross-section

$$\sigma_{\rm R}(s) = \sigma_{\rm peak} \frac{m_\Upsilon^2 \Gamma_\Upsilon^2}{(s - m_\Upsilon^2)^2 + m_\Upsilon^2 \Gamma_\Upsilon^2} \mathcal{B}(\Upsilon \to \gamma a)\,, \tag{5}$$

where m_Υ and Γ_Υ are the mass and width of a specific Υ resonance, and $\sigma_{\rm peak}$ is the peak cross-section defined as

$$\sigma_{\rm peak} = \frac{12\pi \mathcal{B}(\Upsilon \to ee)}{m_\Upsilon^2}\,, \tag{6}$$

with $\mathcal{B}(\Upsilon \to ee)$ being the leptonic branching fraction, experimentally determined for the different $\Upsilon(nS)$ resonances. The effective couplings defined in Eq. (2) appear, instead, in the $\mathcal{B}(\Upsilon \to \gamma a)$ branching fraction, as illustrated in Fig. 2.

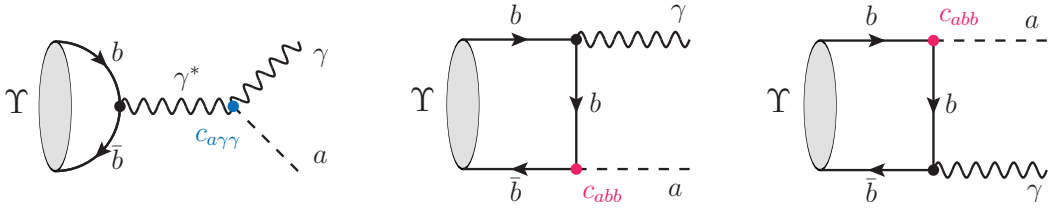

Figure 2 – *Contributions to the $\Upsilon(nS) \to \gamma a$ decays from the effective couplings introduced in the Lagrangian or Eq. ((2)).*

Non-resonant vs Resonant ALP Production. Naively, one would expect that the resonant cross-section (Eq. (5)) clearly dominates over the non-resonant one (Eq. (4)) for the very narrow $\Upsilon(1S)$, $\Upsilon(2S)$ and $\Upsilon(3S)$ resonances, since $\Gamma_\Upsilon/m_\Upsilon \ll 1$. Nevertheless, this turns out to not be the case at B-factories, since these experiments are intrinsically limited by the energy spread of the e^+e^- beam, which is of order $\sigma_W \approx 5$ MeV at current facilities. This value is considerably larger than the width of these resonances, which therefore cannot be fully resolved at B-factories. The only exception is the $\Upsilon(4S)$ resonance, for which $\Gamma_{\Upsilon(4S)} = 20.5$ MeV. Therefore, one should expect a sizable reduction of the estimation in Eq. (5) for the lightest quarkonia resonances, due to this intrinsic experimental uncertainty. To account for the beam-energy uncertainties, the procedure presented in Ref. [11] has been

$\Upsilon(nS)$	m_Υ [GeV]	Γ_Υ [keV]	$\sigma_{\rm peak}$ [nb]	ρ	$\langle\sigma_{\rm R}(m^2_\Upsilon)\rangle_{\rm vis}/\sigma_{\rm NR}$
$\Upsilon(1S)$	9.460	54.02	$3.9(18)\times 10^3$	6.1×10^{-3}	0.53(5)
$\Upsilon(2S)$	10.023	31.98	$2.8(2)\times 10^3$	3.7×10^{-3}	0.21(3)
$\Upsilon(3S)$	10.355	20.32	$3.0(3)\times 10^3$	2.3×10^{-3}	0.16(3)
$\Upsilon(4S)$	10.580	20.5×10^3	2.10(10)	0.83	$3.0(3)\times 10^{-5}$

Table 1: *Estimated visible cross-section at Belle-II for $e^+e^-\to\Upsilon\to\gamma a$ compared to the non-resonant one, $e^+e^-\to\gamma^*\to\gamma a$. Here, vanishing ALP couplings with b-quarks have been assumed, $c_{abb}=0$.*

adopted by performing a convolution of $\sigma_{\rm R}(s)$ with a Gaussian distribution, with spread σ_W,

$$\langle\sigma_{\rm R}(s)\rangle_{\rm vis}=\int{\rm d}q\,\frac{\sigma_{\rm R}(q^2)}{\sqrt{2\pi}\sigma_W}\exp\left[-\frac{(q-\sqrt{s})^2}{2\sigma_W^2}\right]. \tag{7}$$

At the very narrow $\Upsilon(nS)$ resonances, with $n=1,2,3$, one finds $\Gamma_\Upsilon\ll\sigma_W$, in such a way that the previous expression can be simplified by writing [11]

$$\langle\sigma_{\rm R}(m^2_\Upsilon)\rangle_{\rm vis}=\rho\,\sigma_{\rm peak}\,\mathcal{B}(\Upsilon\to\gamma a)\,, \tag{8}$$

where the parameter ρ, defined as

$$\rho=\sqrt{\frac{\pi}{8}}\frac{\Gamma_\Upsilon}{\sigma_W}\,, \tag{9}$$

accounts for the cross-section suppression at the peak due to the finite beam-energy spread.

1.3 The general case: $c_{a\gamma\gamma}\neq 0$ and $c_{abb}\neq 0$

In Table 1, the estimation of the resonant and non-resonant cross-section, for each Υ resonance, along with the peak cross-section $\sigma_{\rm peak}$ and the suppression parameter ρ. This computation has been performed with the Belle-II (KEKB) energy-spread for illustration. From this table, one learns that even though the peak cross-section is large for the $\Upsilon(nS)$ resonances ($n=1,2,3$), the beam-energy uncertainties entail a considerable suppression of the *visible* cross-section. These effects are milder for the $\Upsilon(4S)$ resonance, but in turn the cross-section at the peak is much smaller in this case. The final results are summarized in the last column of Table 1, which shows that the effective resonant cross-section is smaller than the non-resonant one, but it still contributes with numerically significant effects. For the (very) narrow resonances $\Upsilon(nS)$ ($n=1,2,3$), the resonant contribution amounts to corrections between 20% and 50% to the non-resonant one, which should be included when reinterpreting experimental searches. [b] On the other hand, for the $\Upsilon(4S)$ resonance the resonant contribution turns out to be negligible, due to its larger width, as expected.

The previous discussion implies that the resonant contributions are not only important to correctly assess limits on the ALP coupling to photons, $c_{a\gamma\gamma}$, but they also open the window to probe the ALP coupling to b-quarks, c_{abb}. The total $\mathcal{B}(\Upsilon\to\gamma a)$ branching fraction reads [8]:

$$\mathcal{B}(\Upsilon\to\gamma a)\;=\;\frac{\alpha_{\rm em}}{216\,\Gamma_\Upsilon}m_\Upsilon f_\Upsilon^2\left(1-\frac{m_a^2}{m_\Upsilon^2}\right)\left[\frac{c_{a\gamma\gamma}}{f_a}\left(1-\frac{m_a^2}{m_\Upsilon^2}\right)-2\frac{c_{abb}}{f_a}\right]^2. \tag{10}$$

Note, however, that the computation of the c_{abb} contributions are done within a first approximation that considerably simplifies the QCD structure-dependent emission of this decay [12,13]. If a NP signal is indeed observed, a more accurate theoretical calculation would be needed to fully assess the (non-perturbative) effects associated to the last two diagrams in Fig. 2.

[b] Interference effects between the non-resonant and resonant $c_{a\gamma\gamma}$ terms turn out to be negligible due to the small width of the $\Upsilon(nS)$ resonances.

As shown in Eq. (10), the $c_{a\gamma\gamma}$ and c_{abb} couplings can induce comparable contributions to the non-resonant cross-section in Eq. (5). Moreover, depending on the relative sign, these two couplings can interfere destructively or constructively. Finally, note that Eq. (10) shows a different dependence on m_a and $\{c_{a\gamma\gamma}, c_{abb}\}$ than the non-resonant cross-section in Eq. (4).

2 Summary of experimental searches

From the previous discussion, one learns that the non-resonant cross-section, via the coupling $c_{a\gamma\gamma}$, is the largest one, but it can be of the same order of the resonant one, cf. Tab. 1. Moreover, the latter searches have the advantage of being sensitive to both $c_{a\gamma\gamma}$ and c_{abb} couplings. Based on these observations, ALP searches at B-factories can be classified in the following three categories:

i) Resonant searches: Excited quarkonia states $\Upsilon(nS)$ (with $n > 1$) can decay into lighter $\Upsilon(nS)$ resonances via pion emission, as for example $\Upsilon(2S) \to \Upsilon(1S)\,\pi^+\pi^-$ and $\Upsilon(3S) \to \Upsilon(1S)\,\pi^+\pi^-$. By exploiting the kinematics of these processes one can reconstruct the $\Upsilon(1S)$ meson and then study its decay into a specific final state, which can, for instance, be the invisible Υ decay or the Υ decay into photon and a light (pseudo)scalar particle. These searches are dubbed *resonant*, since they allow to directly probe $\mathcal{B}(\Upsilon \to \gamma a)$ in a *model-independent* way, regardless of the non-resonant contribution from Fig. 1. In other words, reported limits on $\mathcal{B}(\Upsilon(1S) \to \gamma a)$ can be used to constrain both $c_{a\gamma\gamma}$ and c_{abb} via Eq. (10). Searches along these lines have been performed, for instance, by BaBar [14] and, more recently, by Belle [15], under the assumption that the ALP does not decay into visible particles inside the detector.

ii) Mixed (non-)resonant searches: Alternatively, experimental searches could be performed at $\Upsilon(nS)$ (with $n = 1, 2, 3$) without identifying the Υ decay from a secondary vertex. Example of such experimental searches are the ones [16] performed at $\sqrt{s} = m_{\Upsilon(3S)}$, where limits on $\mathcal{B}(\Upsilon(3S) \to \gamma a) \times \mathcal{B}(a \to \text{inv})$ are extracted from the total $e^+e^- \to \gamma a(\to \text{inv})$ cross-section. From the above discussion, however, it is clear that this method is probing both resonant (Eq. (8)) and non-resonant (Eq. (4)) cross-sections and therefore model-independent limits on $\mathcal{B}(\Upsilon(3S) \to \gamma a)$ could not be extracted from these experimental results. The only scenarios for which such limits can be derived are the ones with $|c_{a\gamma\gamma}| \ll |c_{abb}|$, as predicted in models with an extended Higgs sector, since the non-resonant cross-section practically vanishes in this case. In the most general ALP scenario, instead, the limits on $\{c_{a\gamma\gamma}, c_{abb}\}$ can be obtained from via a rescaling factor,

$$\frac{\langle \sigma_{\rm R}(s) + \sigma_{\rm NR}(s) \rangle_{\rm vis}}{\langle \sigma_{\rm R} \rangle_{\rm vis}} \approx 1 + \frac{\sigma_{\rm NR}}{\langle \sigma_{\rm R} \rangle_{\rm vis}}\,, \tag{11}$$

which accounts for the non-resonant contributions (Eq. (7)) that have been overlooked experimentally in the total cross-section. Note, also, that similar effects have also been overlooked in reinterpretations of other experimental limits, as for example the ones on $\mathcal{B}(\Upsilon(3S) \to \gamma a) \times \mathcal{B}(a \to \text{hadrons})$ to constrain the product of ALP couplings to photons and gluons. [c]

iii) Non-resonant searches: The resonant cross-section is negligible at the $\Upsilon(4S)$ resonance, as can be seen from Table 1, since its mass lies just above the $B\overline{B}$ production threshold. Therefore, experimental searches at the $\Upsilon(4S)$ resonance can only probe the $c_{a\gamma\gamma}$ coupling via the non-resonant ALP production illustrated in Fig. 1. To our knowledge, no such ALP *invisible* search has been performed yet at B-factories. As an order of magnitude estimation one can use the $\mathcal{B}(\Upsilon(4S) \to \gamma a)$ limits extracted from Belle-II data on $\Upsilon(4S) \to \gamma\, a, a \to \gamma\gamma$ decay [17].

3 Constraining the ALP parameter space

Constraints on the $\{c_{a\gamma\gamma}, c_{abb}\}/f_a$ space are shown in Fig. 3, considering, for illustration, the *invisible* ALP scenario, i.e. by assuming that $\mathcal{B}(a \to \text{inv}) = 1$, or equivalently, that the ALP

[c] The reinterpretation described above has a possible caveat related to the treatment of the background. See Ref. [8] for a detailed discussion on this point.

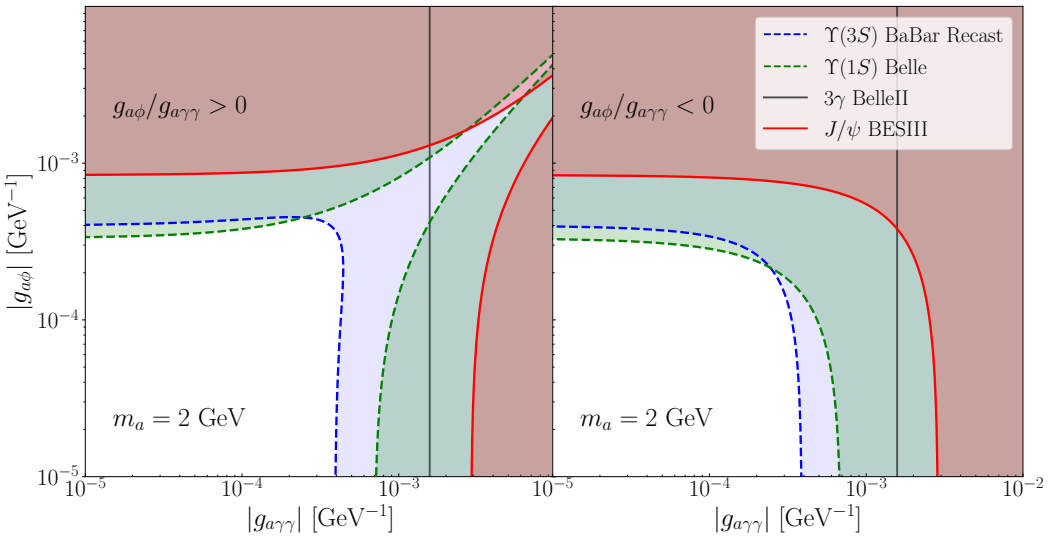

Figure 3 – *Excluded* $\{g_{a\gamma\gamma}, g_{aff}\}$ *parameter space for the invisible scenario with two couplings simultaneously present. Dashed constraints are taken from* [8]. *The red shaded area is derived from the BESIII search* [18] *and the full black line is taken from the Belle-II search* [17]. *Resonant radiative decays of* Υ *and* J/ψ *test different fermionic parameters,* g_{abb} *and* g_{acc} *respectively.*

does not decay inside the detector. Clearly, the results derived below can be easily recast to scenarios in which the invisible ALP branching fraction is smaller than one.

The Left (Right) plot refers to the $c_{abb}/c_{a\gamma\gamma} > 0$ ($c_{abb}/c_{a\gamma\gamma} < 0$) sign choice, for the chosen reference value of $m_a = 2$ GeV. As expected from Eq. 10 for the $c_{abb}/c_{a\gamma\gamma} > 0$, a destructive interference between the fermion and photon ALP coupling can appear. In this case, the $\Upsilon(1S)$ constraints have a flat direction that cannot be resolved by only relying on resonant ALP searches. The combination of couplings that lead to this cancellation depends on the ALP mass, especially for m_a values near the kinematical threshold. BaBar results obtained at the $\Upsilon(3S)$ resonance, which is not reconstructed, depicts, once recasted, a different sensitivity to $\{c_{a\gamma\gamma}, c_{abb}\}$, as shown by the blue regions in the same plot. While a cancellation between $c_{a\gamma\gamma}$ and c_{abb} is possible for resonant cross-section, this cannot occur for the non-resonant one, which depends only on the $c_{a\gamma\gamma}$ coupling. The combination of these complementary searches allows one to corner the ALP parameter space as depicted in Fig. 3. Moreover, projections for searches performed at Belle-II, operating at the $\Upsilon(4S)$ resonance, as computed in Ref. [?], are displayed in the same plot for an expected luminosity of 20 fb^{-1}. As can be seen in Fig. 3, B-Factory and Charm-Factory sensitivities are comparable.

Acknowledgments

This work received funding from the European Union's Horizon 2020 research and innovation programme under the Marie Skłodowska-Curie grant agreement N° 860881-HIDDeN, grant agreement N° 101086085–ASYMMETRY and by the INFN Iniziative Specifica APINE. The work of LDL is also supported by the project "CPV-Axion" under the Supporting TAlent in ReSearch@University of Padova (STARS@UNIPD).

References

1. R. D. Peccei and H. R. Quinn, Phys. Rev. Lett. **38**, 1440 (1977).
2. F. Wilczek, Phys. Rev. Lett. **40**, 279 (1978).
3. S. Weinberg, Phys. Rev. Lett. **40**, 223 (1978).
4. J. E. Kim, Phys. Rev. Lett. **43**, 103 (1979).

5. M. A. Shifman, A. I. Vainshtein and V. I. Zakharov, Nucl. Phys. B **166**, 493 (1980).
6. A. R. Zhitnitsky, Sov. J. Nucl. Phys. **31**, 260 (1980) [Yad. Fiz. **31**, 497 (1980)].
7. M. Dine, W. Fischler and M. Srednicki, Phys. Lett. **104B**, 199 (1981).
8. L. Merlo, F. Pobbe, S. Rigolin and O. Sumensari, JHEP **06** (2019), 091.
9. L. Di Luzio, A. W. M. Guerrera, X. Ponce Díaz and S. Rigolin, In preparation.
10. I. Brivio, M. B. Gavela, L. Merlo, K. Mimasu, J. M. No, R. del Rey and V. Sanz, Eur. Phys. J. C **77**, no. 8, 572 (2017).
11. S. Eidelman, D. Epifanov, M. Fael, L. Mercolli and M. Passera, JHEP **1603**, 140 (2016).
12. A. W. M. Guerrera and S. Rigolin, Eur. Phys. J. C **82** (2022) no.3, 192.
13. A. W. M. Guerrera and S. Rigolin, Fortsch. Phys. **71** (2023) no.2-3, 2200192.
14. P. del Amo Sanchez *et al.* [BaBar Collaboration], Phys. Rev. Lett. **107**, 021804 (2011).
15. I. S. Seong *et al.* [Belle Collaboration], Phys. Rev. Lett. **122**, no. 1, 011801 (2019).
16. B. Aubert *et al.* [BaBar Collaboration], arXiv:0808.0017 [hep-ex].
17. F. Abudinén *et al.* [Belle-II], Phys. Rev. Lett. **125** (2020) no.16, 161806.
18. M. Ablikim *et al.* [BESIII], Phys. Lett. B **838** (2023), 137698.